nature communications

Article

https://doi.org/10.1038/s41467-025-55883-1

Removal of dissolved organic carbon in the West Pacific hadal zones

Received: 24 September 2024

Accepted: 2 January 2025

Published online: 16 January 2025

Check for updates

Mengfan Chu[1,2], Rui Bao[1,2] ✉, Michael Strasser[3], Ken Ikehara[4], Yang Ding[5], Kejian Liu[1], Mingzhi Liu[1], Li Xu[6], Yonghong Wang[7], Piero Bellanova[8], Troy Rasbury[9], Martin Kölling[10], Natascha Riedinger[11], Min Luo[12], Christian März[13,14], Kana Jitsuno[15], Zhirong Cai[16], Cecilia McHugh[17] & Ellen Druffel[18]

The deep oceans are environments of complex carbon dynamics that have the potential to significantly impact the global carbon cycle. However, the role of hadal zones, particularly hadal trenches (water depth > 6 km), in the oceanic dissolved organic carbon (DOC) cycle is not thoroughly investigated. Here we report distinct DOC signatures in the Japan Trench bottom water. We find that up to 34% ± 7% of the DOC in the trench bottom is removed during the northeastward transport of dissolved carbon along the trench axis. This DOC removal increases the overall DOC recalcitrance of the deep Pacific DOC pool, and is potentially enhanced by the earthquake-triggered physical and biogeochemical processes in the hadal trenches. Radiocarbon analysis on representative oceanic transects further reveals that the Pacific deep-water DOC undergoes distinct removal compared to those in the Atlantic and Indian Oceans along the thermohaline transport. Our findings highlight hadal trenches as previously unrecognized DOC sinks in the deep ocean system, with varying dynamics that warrant further investigation.

Deep-sea dissolved organic carbon (DOC) is a major carbon pool that circulates between ocean basins and has been hypothesized to affect past climate changes (e.g., meditating hyperthermal carbon releases in Eocene[1]). The DOC and dissolved inorganic carbon (DIC) in the deep ocean show different radiocarbon (^{14}C) age variations along their transport[2], indicating repeated cycling and longer turnover time of certain DOC fractions[3]. Growing consensus is that the deep-sea DOC pool consists of fractions with different reactivities and residence times, and is thus subject to hidden, dynamic cycling in the contemporary ocean[4,5]. To elucidate the role of deep-sea DOC in the global

[1]Frontiers Science Center for Deep Ocean Multispheres and Earth System, Key Laboratory of Marine Chemistry Theory and Technology, Ministry of Education, Ocean University of China, Qingdao, China. [2]Laboratory for Marine Geology, Qingdao Marine Science and Technology Center, Qingdao, China. [3]University of Innsbruck, Institute of Geology, Innsbruck, Austria. [4]National Institute of Advanced Industrial Science and Technology (AIST), Geological Survey of Japan, Institute of Geology and Geoinformation, Ibaraki, Japan. [5]Frontier Science Center for Deep Ocean Multispheres and Earth System (FDOMES) and Physical Oceanography Laboratory, Ocean University of China, Qingdao, China. [6]NOSAMS Laboratory, Woods Hole Oceanographic Institution, Woods Hole, MA, USA. [7]Department of Marine Geosciences, Ocean University of China, Qingdao, China. [8]RWTH Aachen University, Institute of Neotectonics and Natural Hazards & Institute of Geology and Geochemistry of Petroleum and Coal, Aachen, Germany. [9]Department of Geosciences, Stony Brook University, New York, NY, USA. [10]MARUM – Center for Marine Environmental Science, University of Bremen, Bremen, Germany. [11]Boone Pickens School of Geology, Oklahoma State University, Oklahoma, USA. [12]Shanghai Engineering Research Center of Hadal Science and Technology, College of Marine Sciences, Shanghai Ocean University, Shanghai, China. [13]School of Earth and Environment, University of Leeds, Leeds, UK. [14]Institute for Geosciences, University of Bonn, Bonn, Germany. [15]Department of Life Science and Medical Bioscience, Waseda University, Tokyo, Japan. [16]Department of Geology and Mineralogy, Division of Earth and Planetary Sciences, Graduate School of Science, Kyoto University, Kyoto, Japan. [17]Queens College, City University of New York, School of Earth and Environmental Sciences, New York, NY, USA. [18]Department of Earth System Science, University of California, Irvine, CA, USA. ✉e-mail: baorui@ouc.edu.cn

carbon cycle and climate change, it is crucial to investigate the transport and turnover of DOC on inter- and cross-oceanic basin scales, with both water mass transportation and distinct carbon sources considered.

The deep Pacific Ocean is the terminus of the global thermohaline transport route (e.g., the ocean conveyor belt)[6,7]. The degradation of deep-sea DOC along this transport consequently leads to a less abundant and more refractory DOC pool in the Pacific Ocean compared to the Atlantic and Indian Oceans[5,6,8]. However, previous studies suggested that DOC in the deep Pacific is not solely regulated by thermohaline circulation, but is subject to influences from regional sources and sinks as well[3,4,9]. Specifically, the Pacific Ocean has various geographical units (hadal trenches, seamounts, etc.) with complex bathymetry and biogeochemical processes that can potentially influence the cycling of DOC, leaving gaps in our understanding of the Pacific deep-water DOC dynamics.

The majority of the world's hadal zones (water depth > 6 km) and hadal trenches are found in the West Pacific Ocean, and these are closely involved in the global deep-water circulation[10,11]. Although hadal trenches are considered as relatively isolated bathymetric features with limited connections to the adjacent deep ocean basins, emerging observations suggest active and thorough material exchange between hadal trenches and the open ocean. The Lower Circumpolar Deep Water (LCDW) enters the West Pacific trench system via the Mariana Trench[12] (Supplementary Fig. 1a). Within the West Pacific trench continuum, thorough water ventilation is further suggested by the oxygen-rich trench bottom waters[11]. Water exchange with the deep Pacific shape the biological and chemical environments in the trench[13], while contributions of hadal trenches to the deep-sea biogeochemical cycle remain unexplored.

The distinctive ultra-deep-water conditions, drastic topography and dynamic carbon cycling render the West Pacific hadal trenches as potential loci for deep-sea DOC turnover. Inside the trenches, the topographic relief regulates deep-sea currents and drives vertical mixing[11,14], facilitating DOC exchange with the open ocean. Frequent earthquakes transport particulate organic carbon (POC) into the hadal trenches via turbidity currents[15,16]. Repeated exposure of POC to oxic environments (e.g., water column and surface sediment) leads to intensive microbial degradation and high OC turnover rates[17,18]. These dynamic biogeochemical conditions distinguish the hadal trenches from other abyssal and hadal environments[19]. While emerging studies investigated the OC cycling in the trench sediments[18,20,21], fewer evaluates the contribution of hadal trenches to the upper water column, especially the role of hadal DOC cycling in thermohaline circulation.

During the International Ocean Discovery Program (IODP) Expedition 386, bottom water and surface sediments were collected along the Japan Trench axis (Fig. 1a), which represents the first coordinated research effort to sample a hadal trench in high spatial resolution[22]. In this study, we examine the concentration, stable and radiocarbon isotopic signatures of DOC and DIC in the bottom water, and POC in the surface sediments in the Japan Trench (Fig. 1b). Our objectives are to better understand the contribution of the trench to West Pacific DOC cycling, and to explore the role of oceanic hadal zones in global thermohaline circulation.

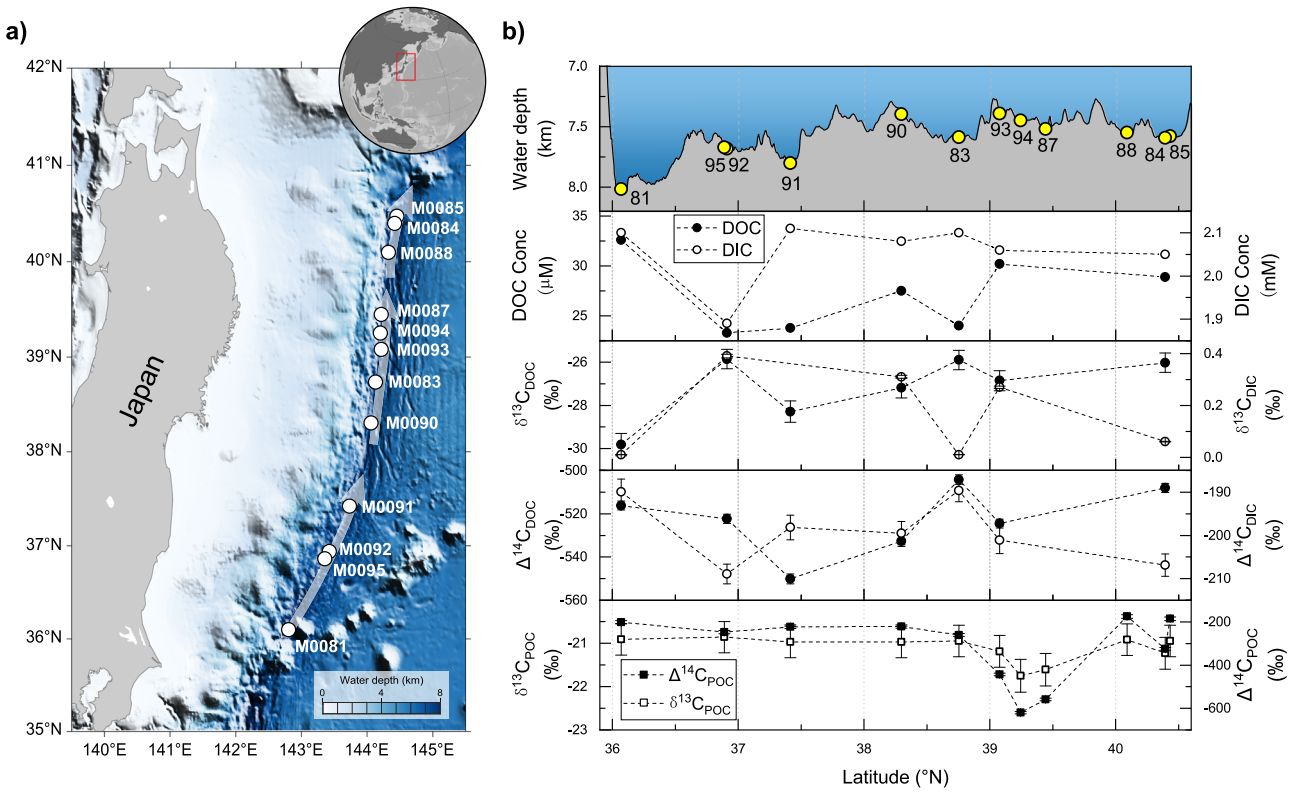

Fig. 1 | The concentration and characteristics of the dissolved carbon in the Japan Trench bottom water and particulate organic carbon (POC) in the surface sediments. a Locations of the study sites. The white arrow indicates the direction of bottom current[36]. The figure is generated using MATLAB (v2023) and Ocean Data View (Schlitzer, R., http:// odv.awi.de). The bathometry data is from ETOPO 2022 15 Arc-Second Global Relief Model[64]. **b** The water depths, concentrations, $\delta^{13}C$ and $\Delta^{14}C$ values of the bottom water (below 7.3 km water depth) dissolved organic and inorganic carbon (DOC, DIC) in the Japan Trench, and the $\delta^{13}C_{POC}$ and $\Delta^{14}C_{POC}$ values of the surface sediments. Error bars indicate measurement errors. All dissolved carbon data from this study is presented in Supplementary Table 2 and Source Data file.

Results and discussion

Trench water connectivity and dissolved carbon characteristics

The water connectivity between West Pacific hadal trenches has been confirmed by observational studies[12,23]. Calculated potential density anomalies (referred to 4000 dbar in kg/m^3, σ_4 = 45.28–46.08, see Method) of the Japan Trench bottom waters align with those at near-hadal depth in the Japan Trench[24] (σ_4 = 45.86), implying ventilation between the trench bottom and upper water columns. Deep-sea currents enter the West Pacific trenches mainly via LCDW[12], and is presumed to have dissolved carbon with characteristics resembling those in the open ocean. Indeed, the $\Delta^{14}C_{DIC}$ values in the Japan Trench bottom water (range from −209‰ to −190‰, Fig. 1b) resemble the deep water $\Delta^{14}C_{DIC}$ values in the West Pacific (−205‰ to −183‰ below 5 km water depth[25]) and the Mariana Trench (−203‰ to −201‰ below 5 km water depth[26]), but are higher than those in the Philippine Sea (−221‰ to −196‰ below 4 km water depth[27]). This $\Delta^{14}C$ variation is consistent with the water transport route in the West Pacific, where a branch of LCDW moves northward along 145°E, while another branch enters the Philippine Sea through the Mariana-Yap Trench Junction[10] (Supplementary Fig. 1a). Hence, the properties of the Japan Trench bottom water DIC suggest that the Japan Trench has water exchange with the open ocean[11,28,29].

The trench-scale $\Delta^{14}C_{DIC}$ variation may be subject to dynamic processes, as suggested by the highly-variable concentrations and $\Delta^{14}C_{DIC}$ values (Fig. 1b). Based on the age difference (170 ^{14}C years, Fig. 1b) between the bottom water DIC at IODP Sites M0081 and M0084, a rough estimate of bottom current velocity would be about 0.01 cm/s to travel the distance of ~400 km between the sites. However, the observed current velocity in the West Pacific trenches ranges from 0.1 cm/s (Mariana Trench, 10 km water depth) to 9 cm/s (Kermadec Trench, 6 km water depth[11]), all of which exceed our bottom current velocity estimated using $\Delta^{14}C_{DIC}$ by 1–2 orders of magnitude. Within the Japan Trench, the estimated velocity using $\Delta^{14}C_{DIC}$ is much lower than the modeled (~2 cm/s, Supplementary Fig. 1b) and observed northward deep current velocity in the Japan Trench (3–7 cm/s[30]).

The trench DOC pool, in the meantime, exhibits more significant $\Delta^{14}C$ variation (from −504 to −550‰) than the DIC pool. The $\Delta^{14}C_{DOC}$ variation along the trench is larger than that of the P16N transect[31] across the central Pacific (from −514‰ to −548‰). The $\delta^{13}C$ and $\Delta^{14}C$ variations of bottom water and porewater DOC indicate that the influence of POC remineralization on the bottom water DOC pool is relatively small. Along the Japan Trench, the bottom water DOC is much older and ^{13}C-depleted than porewater DOC (Supplementary Fig. 2), but are rather more similar with the Mariana Trench and the Pacific deep-water DOC (Supplementary Fig. 2). Hence, the majority of the bottom water DOC is also transported into the Japan Trench by the Pacific deep currents, and received a relatively small influence from porewater DOC pool.

DOC removal and alteration in the Japan Trench bottom water

The average DOC concentration we observe in the Japan Trench bottom water (27.2 ± 3.6 μM (avg. ± std., n = 7), Fig. 1b) is very low in comparison to the near-hadal zones in central Pacific Ocean, where DOC concentration typically ranges from 35 to 42 μM[8,32]. This significant DOC deficit is not observed in the Izu-Bonin and Mariana Trenches, where DOC concentrations reach 38 μM[26,33]. Especially, the $\delta^{13}C_{DOC}$ values in the Japan Trench bottom water (from −25.9‰ to −29.8‰, Fig. 1b) are within the range reported for the low molecular weight, hydrophilic DOC fraction (from −23.9‰ to −31.5‰) in the north[2] and northeast Pacific Ocean[34]. Compared to the bulk DOC, the low molecular weight DOC is generally more depleted in ^{14}C and mainly comprise of refractory compound[35]. These comparisons suggest that the Japan Trench bottom water DOC pool may consist of components that have survived extensive degradation in the hadal trench environments. In the meantime, the DIC concentrations in the Japan Trench bottom water (2.056 ± 0.076 mM, Fig. 1b) are also lower than the deep-water DIC in the Mariana Trench (2.178 mM at 8.72 km water depth[26]), suggesting that all the dissolved carbon fractions are significantly removed in the Japan Trench. The fact that no continuous decline of DOC concentration is observed along the trench axis indicates independent DOC removal process within each basin. This may be caused by limited exchanges between the bottom and the deep waters[36], temporal variation of the trench current[37], and locally-varying OC cycling among the trench basins (Supplementary Text 1).

The DOC removal process has been documented in various deep ocean settings, including oceanic crust[38], the Mediterranean Sea[39], and hydrothermal plumes[34]. Previous study suggested that the deep Pacific DOC pool (35–40 μM in total) may contain up to 30% semi-labile DOC (7–12 μM), which are subject to quick turnover[5]. In hadal trenches, the rapid deposition and intensive resuspension of sediments triggered by submarine earthquakes can stimulate microbial activity[17] and alter benthic microbial communities[40], which potentially lead to microbial priming and consequently, deep-water DOC removal[9,41]. The DOC removal via microbial processes can be accompanied by DIC removal through authentic carbonate precipitation in the Japan Trench sediments[42]. The cascade of dissolved carbon removal in the Japan Trench thus suggests that the hadal trench have the potential to sequester more carbon than expected.

Spatially-varying DOC removal is evident at regional scales along the Japan Trench axis and may be linked to specific local depositional environments (Supplementary Text 1). Significant variations in trench topography can induce vigorous vertical and horizontal mixing (Supplementary Fig. 1b), promoting exchange between bottom and deep waters and enhancing DOC removal in the trench bottom waters. For instance, Sites M0083, M0091, and M0092, located in the deeper Japan Trench basins compared to other sites, exhibit particularly low DOC concentrations (Supplementary Text 1). Topography of these deeper basins may prolong the residence time of the water mass and thus foster more intensive DOC removal. Moreover, different extents of connections to continental margin via submarine canyons (i.e., Ogawara and Nakaminato Canyons[43]) along the Japan Trench may further add to the spatial variability of DOC input and removal within the trench. The West Pacific trench continuum comprises a series of trenches with various environmental conditions (topography, earthquake frequencies, connectivity with land, etc.). It is therefore reasonable to expect different extents of DOC removal in the West Pacific trenches (the Mariana, Izu-Bonin and Kuril Trenches, etc., Supplementary Fig. 3) regulated by different environmental settings. Overall, the observed DOC deficit in the Japan Trench bottom water highlights the need to further investigate the removal mechanisms, which are likely linked to the microbial processes, earthquake occurrences and depositional environments in the hadal trenches.

Contribution of Pacific hadal zones to the global DOC cycle

The DOC removal processes in hadal zones were not considered in current global estimates of DOC turnover. Although the trench DOC pool is small compared to the open ocean, our above findings demonstrate that the hadal trenches are potential reactors of DOC that act as efficient sinks to the Pacific DOC pool (Supplementary Fig. 3). Importantly, the Pacific hadal DOC pool potentially undergoes various alterations at different spatial scales. By applying the "Keeling plot" perspective[44,45], and dividing the marine DOC pool into a refractory background component (Fraction modern = 0) and a labile, modern component (Fraction modern > 0), a plot of the modern DOC (c × Fraction modern) vs. the total DOC concentrations can show the addition or removal of the excess DOC fractions in the global oceans (Fig. 2). In this plot, the DOC pools with similar biogeochemical source-sink fates define one mathematic regression line (see Method). For instance, the global surface ocean DOC pools show a consistent linear

https://doi.org/10.1038/s41467-025-55883-1

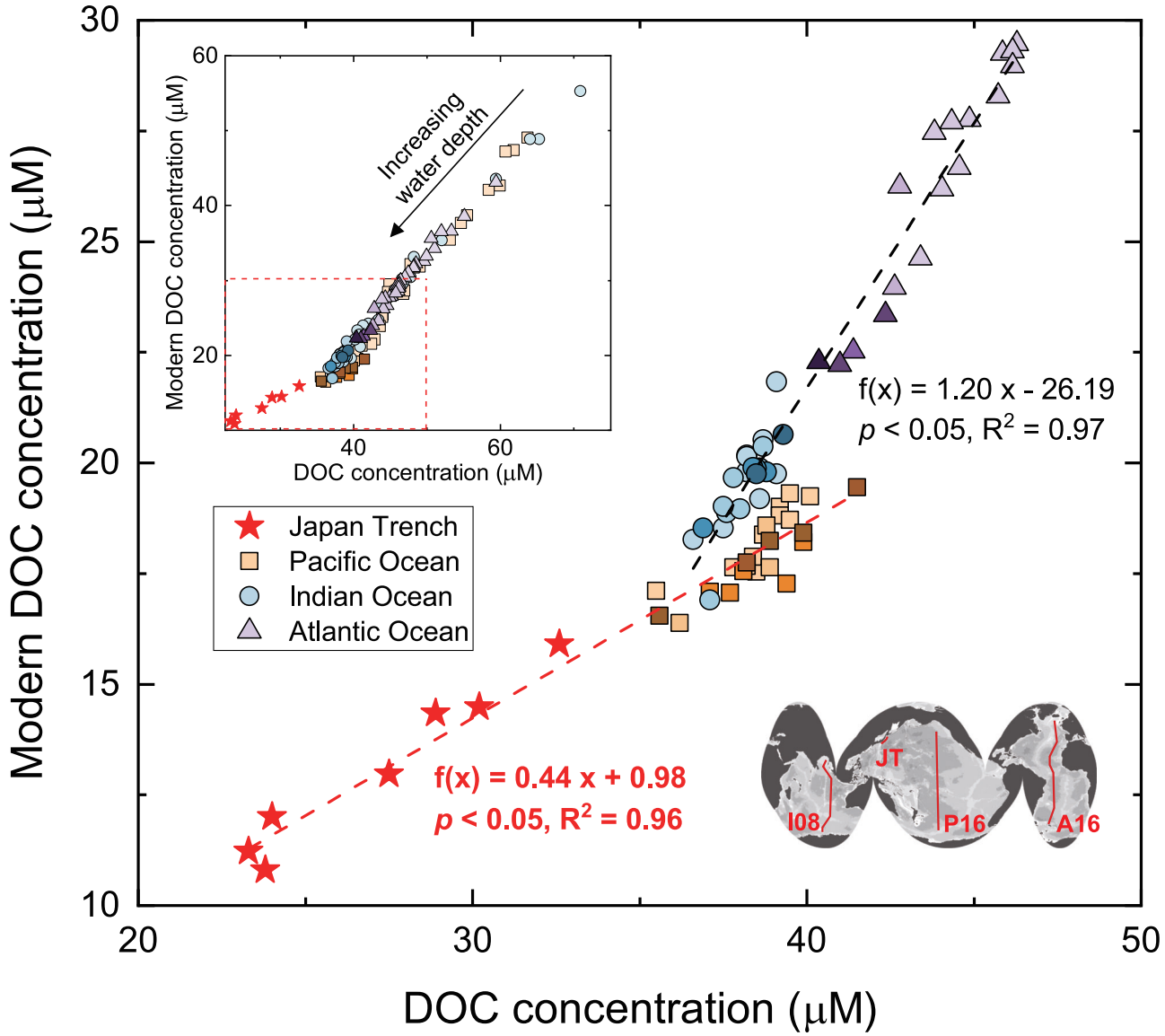

Fig. 2 | Dissolved organic carbon (DOC) fates in the Atlantic, Indian, Pacific Oceans (purple, blue and orange symbols, respectively) and in the Japan Trench (red symbols) indicated by the modern DOC *vs.* total DOC concentrations. Modern DOC concentration is calculated by multiplying DOC concentration by Fraction modern (i.e., the activity ratio of the sample relative to a modern reference material), and indicates the concentration of recently synthesized, excess DOC component in the total DOC pool. Different symbols represent DOC pools in the Atlantic (World Ocean Circulation Experiment (WOCE) transects A16, $n = 34$), Indian (WOCE transect I08, $n = 45$), Pacific (WOCE transect P16, $n = 53$) Oceans[27] and Japan Trench (JT, $n = 7$, this study).

relationship (Fig. 2, inserted figure), indicating similar source-sink mechanisms in the shallow (above 1 km water depth) Atlantic, Indian and Pacific Oceans. However, the fate of DOC in deep-water (below 1 km water depth) environments is subject to more complex processes as suggested by the high variation and discrepancy between the three oceans (Fig. 2). The deep-water DOC pools in the Atlantic and Indian Oceans follow one trend, while those in the Pacific Ocean (including the Japan Trench) follow another (Fig. 2). Especially, the data in the Japan Trench shows better agreement with those in the deep Pacific Ocean (stars and octangles in Fig. 2, respectively). This suggests that DOC removal processes may universally occur in the hadal Pacific Ocean.

The oceanic DOC pool is affected by unidentified removal processes in the world's oceans[4]. A basin-wise analysis[9] concluded that the DOC in the deep Pacific remains conservative during most of the transports, but only intensively removed in regional sinks (i.e., in the northern Pacific Ocean below 3 km water depth). Our observation at the extreme depths of hadal trenches contributes to understanding the mechanisms by which DOC is removed in the north Pacific Ocean as part of the thermohaline circulation. According to the mass-balance calculation (Method and Table 1), the removed DOC fraction at most sites (excluding Site M0081) would have isotopic characteristics consistent with semi-labile, marine DOC ($\delta^{13}C = -15‰$; Table 1). Our calculation also indicates that approximately 34% (13 μM) of the DOC entering the West Pacific trenches is removed during its transit through the Japan Trench (Table 1). Using the minimum velocity of 0.1 cm/s in the Mariana Trench[11], it takes approximately 13 years for the bottom water to traverse along the Japan Trench axis (400 km). The 13 μM DOC removal thus derives approximately 1 mol C/kg/yr, which falls between the ranges of semi-labile (2–9 μmol/kg/yr) and semi-refractory DOC removal rates (0.2–0.9 μmol/kg/yr)[4], and agrees with our binary mixing model, in which the removed DOC fraction has a $\delta^{13}C$ value of −15‰ (Table 1). The observed DOC removal in the Japan Trench is thus comparable to global estimations in relatively short time over small transport distance. Through trench connections and water upwelling, part of the LCDW returns to the open ocean at the far

end of north Pacific[24] (Fig. 3) and eventually join the Pacific Deep Water. The altered DOC pool from the deepest part of the Pacific Ocean, with reduced concentration and increased recalcitrance, may thus reflect a previously undiscovered DOC turnover mechanisms in the ocean (Supplementary Fig. 4 and Supplementary Table 1).

Overall, our results highlight the Pacific hadal trench system as a previously unrecognized DOC sink and underscore the need to investigate the DOC cycling in oceanic hadal zones. The role of DOC cycling in the hadal zones has not been thoroughly investigated in the classical ocean conveyor belt theory, primarily due to technical constraints. The processes involved in DOC removal in hadal zones contribute to the overall recalcitrance of the deep-sea DOC pool through mechanisms that may vary both temporally and spatially. Conversely, the observed net removal of DOC in hadal environments may arise from complex interactions, including the consumption, addition, and transformation of specific DOC fractions. Our findings in the hadal trench suggest the presence of underlying processes within the DOC cycling associated with thermohaline transport, underscoring the necessity to explore the hadal DOC cycles. Moreover, the DOC removal in the hadal trenches indicates that global DOC cycling is not solely governed by processes in the oceanic water column, but also indirectly influenced by solid-Earth processes (e.g., earthquakes) in the subduction zones. This points to a crucial role of earthquake-triggered processes in hadal environments in connecting tectonic activities on geological timescales with millennial-scale carbon cycling in the contemporary ocean. A comprehensive understanding of dissolved carbon dynamics in the deepest ocean regions is therefore essential for elucidating the historical and future implications of Earth's carbon storage and its implications for climate change.

Table 1 | DOC removal proportions in the Japan Trench sites

Site	f_1	f_x	$\delta^{13}C_x$ (‰)	$\Delta^{14}C_x$ (‰)	Removal proportion
M0081	82%	19%	8	−618	19%
M0083	60%	40%	−18	−581	40%
M0084	72%	28%	−15	−605	28%
M0090	69%	31%	−13	−540	31%
M0091	60%	41%	−15	−513	41%
M0092	58%	42%	−19	−553	42%
M0093	76%	25%	−11	−567	25%
Average ± STD	66% ± 7%	34% ± 7%	−15 ± 3	−560 ± 12	34% ± 7%

f_x and f_1 represent the relative proportions of the removed and remaining DOC fractions, respectively. $\delta^{13}C_x$ and $\Delta^{14}C_x$ represent the $\delta^{13}C$ and $\Delta^{14}C$ values of the removed DOC, respectively. Result of Site M0081 is excluded from average calculation due to other potential mechanisms as discussed in Supplementary Text 1.

Methods

Research materials

The Japan Trench is formed by the Pacific plate subducting beneath the Okhotsk plate at a convergence rate of 80–86 mm/yr[46]. The trench axis forms along the NNE-SSW direction (Fig. 1a), with the northern end

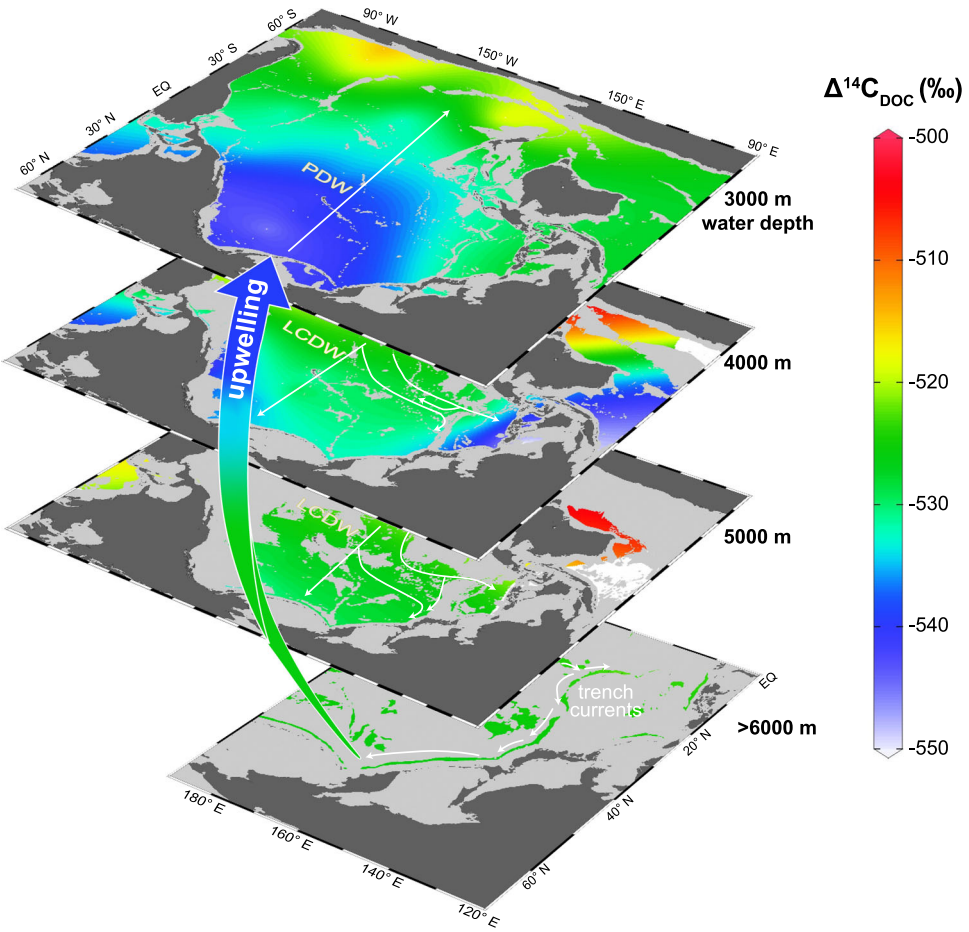

Fig. 3 | Distribution of dissolved organic carbon $\Delta^{14}C$ values in the Pacific. Data in open Pacific are from a compilation of sources[2,3,27,31,65–71]. Data in the hadal trenches are from Mariana Trench[26] and Japan Trench (this study). LCDW Lower Circumpolar Deep Water, PDW Pacific Deep Water. This figure is created with Ocean Data View (Schlitzer, R., http:// odv.awi.de).

intersecting with the Kuril Trench at Erimo Seamount, and the southern end intersecting with the Izu-Bonin Trench at Daiichi Kashima Seamount[47]. The water depth of the trench axis increases southward, from 6.8 km in the north to > 8 km in the south[43]. Due to flexural bending of the subducting plate, the Japan Trench has rough topography with trench- and graben-fill basins at the axis with vertical relief of a few hundreds of meters[48]. These basins effectively preserve the laterally-transported POC[43], resulting in relatively high sedimentation rate (100 and 440 cm/kyr, including the turbidite deposits[49]) in the Japan Trench.

Although limited deep-water circulation inside each trench cannot be ruled out[36], the deep-water exchange between the Izu-Bonin, Japan, Kuril, and Aleutian Trenches serves as a major deep current connecting the west and east Pacific[28]. Opposite currents exist on the landward and oceanward slopes along the trenches[30], with a southward flow on the landward slope and a stronger, faster northward flow on the oceanward slope[23,24,28,30]. The northward flow in the Japan Trench originates from LCDW that enters the Izu-Bonin Trench from the south and the east[36]. This explains the current structure resemblance between the Japan Trench and Izu-Bonin Trench[23].

This study used the bottom water and surface sediments from the Japan Trench collected during IODP Expedition 386. Sediment cores were collected using a Giant Piston Coring (GPC) System from 13 April–1 June 2021 on *R/V Kaimei*[22]. Surface sediments (top 0–3 cm) were sub-sampled from a pilot corer of the GPC system during 13 November–30 November 2022 on *R/V Chikyu* with a spatula and stored inside pre-combusted aluminum foil at −20 °C. After the pilot core was recovered, it was kept in an upright position to allow sampling of bottom water. Bottom water was then collected from inside the core liner above the mudlines using a bottom water sampling system and siphoned into sample bottle. The sampling system consists of a Duran bottle and vacuum pump unit connected by tubes. A tube was placed in the overlying water of the trigger core, and bottom water samples were sucked into the Duran bottle under negative pressure. Bottom water samples were split for DOC (1 L) and DIC (5 mL) measurements. Sample splits were added with 1 mL 10% HCl and stored at −20 °C for DOC measurement, and with 10 μL saturated $HgCl_2$ and stored at 4 °C for DIC measurement. Before further analysis, water samples were filtered through a pre-combusted GF/F filter (0.45 μm). Although diffusion of sediment porewater into the bottom water during sample collection is inevitable due to sampling method, the ammonium concentrations in all bottom water samples used in this study is close to zero and much lower than in the porewater samples (Supplementary Table 3), indicating that porewater diffusion caused minor impacts on the geochemical signals in the bottom water. The water samples were visually clear and contained relatively little POC, also indicating minor disturbance from the resuspended sediments during sample collection.

Analytical methods

Bottom water DOC and DIC were analyzed for concentration, ^{13}C and ^{14}C at the National Ocean Sciences Accelerator Mass Spectrometry Facility (NOSAMS), Woods Hole Oceanographic Institution flowing standard protocols[50,51]. A quartz reactor was prefilled with Milli-Q water and irradiated with UV for 1.5 h before analysis to reduce potential contribution of extraneous carbon. For DOC measurement, the reactor was then added with 2 mL water sample and 0.4 g 33% ultra-pure hydrochloric acid. The joints are then sealed with 85% phosphoric acid. DIC is then purged with ultra-high purity helium (UHP He) at 200 mL/min for 75 min. DOC samples were then irradiated with UV for 3 h, after which the generated CO_2 was purged by UHP He at 120 mL/min for 66 min. The produced CO_2 was then cryogenically trapped, purified, quantified by a manometer, and flame-sealed in a 6.4 mm OD Pyrex glass tube. The quartz reactor on the DOC line was then replaced by a gas-washing device equipped with an injection port to extract DIC. Before sample injection, the device was added with Milli-Q water and phosphoric acid, and then cleaned with UHP He. Samples were irradiated with UV for 3 h, and the generated CO_2 was purged by UHP He at 120 mL/min and collected by a CO_2 trap and manometrically quantified.

$\delta^{13}C$ values were measured by a VG Optima or VG prism Isotope Ratio Mass Spectrometer and reported in ‰ relative to the VPDB standard. ^{14}C was measured by a continuous-flow accelerator mass spectrometer system constructed around an accelerator (National Electrostatics Corporation, Middleton, WI, model 1.5SDH-1) at NOSAMS[50,51]. All ^{14}C data are reported as ^{14}C ages and $\Delta^{14}C$ values[52]. AMS uncertainty was calculated as the larger of either the statistical uncertainty using the total number of ^{14}C counts measured for the target, or an uncertainty calculated from the reproducibility of multiple measurements of the target, both propagated with uncertainties from the normalizing standards and blank subtraction. The DOC procedural blank of UV oxidation method at NOSAMS is 11.0 ± 2.75 μg C (which converts to 0.92 ± 0.23 μM C given the sample volume of 1 L). The $\delta^{13}C$ and Fm values of the procedural blank are −31.0 ± 5.5‰ and 0.14 ± 0.10, respectively (determined by secondary standards OX-II (n = 32) and glycine (n = 30) measurements[50,51]). The reported data in this study have all been corrected by the procedural blank. We applied a relative measurement error of 1.73% for our samples, which is calculated from measurement results of glycine (a standard deviation of 0.5‰ derived from an average of −43‰[50]).

An inter-lab comparison of DOC and DIC $\delta^{13}C$ values[52] provides a premise that the measurement errors of seawater samples are relatively low (0.47‰, n = 5 for DIC and 0.85‰, n = 2 for DOC) between different sample treatments, gas production, and transfer techniques. Additionally, more efforts were made to guarantee the data robustness in this study. First, the volumes and DOC concentrations of our samples exceed the recommendation at NOSAMS (> 900 mL and > 25 μM), therefore help to avoid influences of counting statistics and process blank on small-sized samples. Relatively large sample volume also prevents potential fractionation between the gaseous and dissolved phases of the CO_2 produced by UV oxidation[52]. Second, data comparisons were made between the samples measured in the same batches, and between our data and published data measured at NOSAMS. The bottom water DOC and DIC (Receipt number #175856–#175876) were measured from 1 February–2 February, 2022. We compared the $\delta^{13}C_{DOC}$ values from sediment interstitial water in the Japan Trench (Supplementary Fig. 2 and reference within), which was measured in the same batches at NOSAMS (Receipt number #175877–#176913, from 3 February 3 to 9 May, 2022) with much smaller volumes (8 mL for DOC and 2 mL for DIC). The range of sediment interstitial water $\delta^{13}C_{DOC}$ values is −21.86‰ to −11.29‰[42], which falls within a reasonable range of $\delta^{13}C_{DOC}$ values in marine sediments (e.g., Santa Barbara Basin[53] and Chinese Marginal Seas[54]). Therefore, the large discrepancy between DOC in the bottom water (this study) and sediment interstitial water (Supplementary Fig. 2) is not caused by potential contamination and fractionation during measurements. On the other hand, reasonable and robust results were reported by previous studies that conducted DOC sample measurements at NOSAMS[5,34,39]. Especially, Santinelli et al. reported low $\delta^{13}C_{DOC}$ values observed in the Mediterranean Sea with adequate explanations[39].

Analytical challenges during DOC measurement may interfere with results, for instance, gas break-through during collection after UV irradiation may lead to lower DOC concentration. A comprehensive assessment reported that the gas break-through might result in a 3–4 μM loss of DOC concentration[55]. Hence, this influence does not counteract the significance of the low DOC concentration observed in the Japan Trench bottom water, which is averagely 11–13 μM lower than open ocean deep water. On the other hand, potential influences of pore water diffusion from sediments are discussed in the main text. Briefly, pore waters in the Japan Trench sediments are abundant in

DOC (mM in pore water, instead of μM in bottom water), which is relatively ^{13}C-enriched (Supplementary Fig. 2). Diffusion of such pore water into the bottom water would increase the DOC concentration and decrease the $\delta^{13}C_{DOC}$ values, which were in contrast to our observation. Therefore, we can confidently consider the less abundant and ^{13}C-depleted DOC in the Japan Trench bottom water robust for data interpretation.

For POC samples, freeze-dried bulk sediments were HCl-fumigated at 60 °C for 72 h, followed by NaOH-fumigated at 60 °C for 72 h to neutralize the excess acid[56]. TOC contents were measured by an elemental analyzer (EA-IsoLink, Thermo Fisher Scientific, Bremen, Germany) at Ocean University of China. Samples were weighed into tin capsules before introduced into the EA. The single combustion/reduction reactor of the EA is maintained at 980 °C, with the helium flow at 180 mL/min and the oxygen flow at 250 mL/min, and an O_2 injection end time of 5 s. $\delta^{13}C$ and $\Delta^{14}C$ values were measured at NOSAMS. Samples were weighed into tin capsules and combusted in the EA at 1025 °C. The generated CO_2 was then trapped and separated from the helium carrier gas. Approximately 7% of the gas was taken for $\delta^{13}C$ measurement via an isotope ratio mass spectrometer. The remaining gas was reduced with H_2 to graphite and was taken for measurement via an accelerator mass spectrometer by standard procedures at NOSAMS[57].

Bottom water density calculation

Potential density anomaly referred to 4000 dbar (σ_4 in kg/m^3) of the bottom water in the Japan Trench is calculated by the following equation:

$$\sigma_4 = \rho(T, S, P) - 1000 \quad (1)$$

Where ρ is seawater density (in dbar), T is water temperature (in °C), S is salinity, and P is water pressure (in dbar). The average temperature of two sites in the Izu-Bonin Trench[58], which has similar current structure and water exchange with the Japan Trench[23], was used for T. Salinity data measured on board after sample collection was used for S. Pressure and water depth data of the Pacific Ocean from GLODAPv2.2023 database[59] were fitted to obtain a linear function, that was then used to convert the water depths to pressure (P) at the Japan Trench Sites. Seawater density ρ was then calculated by the International Equation of State of seawater (EOS-80[60]) using the Seawater package in MATLAB. Note that the use of alternative data in the Izu-Bonin Trench may affect the accuracy of our estimated density in the Japan Trench, which should be treated with caution when compared to in-situ data. Data used for calculations is listed in Supplementary Table 4.

Hadal circulation modeling

The mean hadal circulation in the Japan trench shown in Supplementary Fig. 1b is derived from OFES (Ocean General Circulation Model for the Earth Simulator[61,62]. This ocean model is based on Modular Ocean Model ver.3[63], a hydrostatic ocean model subject to Boussinesq and hydrostatic approximations developed by GFDL/NOAA. The model domain covers a near-global region extending from 75°S to 75°N in global oceans, excluding the Arctic Ocean. The model has a horizontal resolution of 1/10° and has 54 layers in the vertical direction with a maximum depth of 5900 m. The mean hadal circulation was computed by averaging the bottom circulation of the OFES model over the time period from 1950 to 2012. The data was obtained from Asian-Pacific Data-Research Center of the IPRC (https://apdrc.soest.hawaii.edu/datadoc/ofes/ofes.php). The water volume transported through the selected trench transects in the West Pacific Ocean is calculated based on the average current data from 1950 to 2012 by the OFES model.

Modern DOC vs. total DOC concentrations

The covariance in DOC concentration and its $\Delta^{14}C$ values during transport across ocean basins can be explained by a Keeling plot model[44,45], which assumes an old background DOC pool mixed with a modern, excess DOC pool along transport. The concentration and Fraction modern value (Fm, the activity ratio of the sample relative to a modern reference material) of the DOC in a water mass can be described as:

$$c = c_{bg} + c_{ex} \quad (2)$$

$$Fm = (Fm_{bg} \times c_{bg} + Fm_{ex} \times c_{ex})/c \quad (3)$$

Where c, c_{bg}, and c_{ex} refer to the concentrations of total DOC, background DOC and excess DOC fractions, and Fm, Fm_{bg}, and Fm_{ex} refer to the Fm values of total DOC, background DOC and excess DOC fractions. Combining Eqs. (2) and (3), we have a binary mixing model:

$$Fm \times c = Fm_{ex} \times c + (Fm_{bg} - Fm_{ex}) \times c_{bg} \quad (4)$$

By assuming that the background DOC fraction in a water mass is refractory, and that its concentration and Fm remain constant during transport, a plot of modern DOC concentration (Fm × c) *vs.* total DOC concentration (c) would be linear. In other words, if the water masses contain a similar amount of background DOC, and that their excess DOC fraction is supplemented or removed with similar mechanisms (i.e., have similar fates), the DOC pools in these water masses would define one linear trend. Different linear trends between groups of data therefore indicate that the DOC in the water mass undergoes different addition/removal processes along transport.

DOC removal proportion in the Japan Trench

The amount and characteristics of the removed DOC in the Japan Trench can be estimated by a two end-member mixing model:

$$f_r = c_r/c_0 \quad (5)$$

$$f_x = c_x/c_0 \quad (6)$$

$$\delta^{13}C_r \times f_r + \delta^{13}C_x \times f_x = \delta^{13}C_0 \quad (7)$$

$$\Delta^{14}C_r \times f_r + \Delta^{14}C_x \times f_x = \Delta^{14}C_0 \quad (8)$$

Where c_r, c_x and c_0 represent the concentrations of the residual, removed and initial DOC pools, respectively. f_r and f_x represent the relative proportions of the residual DOC fraction and the removed DOC fraction, respectively. $\delta^{13}C_r$, $\delta^{13}C_x$, and $\delta^{13}C_0$ represent the $\delta^{13}C$ values of the residual, removed, and initial DOC pool, respectively. Similarly, $\Delta^{14}C_r$, $\Delta^{14}C_x$, and $\Delta^{14}C_0$ represent the $\Delta^{14}C$ values of the residual, removed, and original DOC pool, respectively.

We used the deep-water (water depth = 10 km) DOC concentration (40 μM), $\delta^{13}C$ and $\Delta^{14}C$ values (−22.9‰ and −535‰, respectively) in the Mariana Trench[26] as the initial state of the DOC in the West Pacific trench continuum, where the open ocean DOC enters the trench continuum via LCDW. The DOC concentration, $\delta^{13}C$ and $\Delta^{14}C$ values in each site in the Japan Trench are used as c_r, $\delta^{13}C_r$, and $\Delta^{14}C_r$, respectively. f_x, $\delta^{13}C_x$, and $\Delta^{14}C_x$ can thus be calculated and are presented in Table 1.

DOC pool size estimation in the Pacific hadal zones

The size of the DOC pool in the Japan Trench region (36°N–41°N, 142°E–145°E) was calculated using the following steps. First, the water

volume in each depth zone was calculated using the 3D Analyst function in ArcGIS. Second, the profile of the vertical DOC distribution in the west Pacific was estimated based on WOCE P02 transect (30°N–33°N, 133°E–180°E[27]). The DOC concentration variation with depth was well described by an exponential function ($R^2 = 0.98$, Supplementary Fig. 5). DOC pool size was then estimated by integral calculation of the water volume and DOC concentration in each depth zone. In the hadal zone, two DOC concentrations were used to derive upper and lower limits of the DOC pool size estimation. The integrated DOC concentration at hadal depth in Supplementary Fig. 5 (37.80 μM) was used for the upper limit, and the average DOC concentration observed in the Japan Trench (27.19 μM) was used to derive a lower limit.

Data availability

All data generated in this study are provided in the Supplementary Information and Source Data file. The data in this study are available in Figshare database (https://doi.org/10.6084/m9.figshare.28028723). Source data are provided with this paper.

References

1. Sexton, P. F. et al. Eocene global warming events driven by ventilation of oceanic dissolved organic carbon. *Nature* **471**, 349–353 (2011).
2. Zigah, P. K. et al. Allochthonous sources and dynamic cycling of ocean dissolved organic carbon revealed by carbon isotopes. *Geophys. Res. Lett.* **44**, 2407–2415 (2017).
3. Druffel, E. R. M. & Griffin, S. Radiocarbon in dissolved organic carbon of the South Pacific Ocean. *Geophys. Res. Lett.* **42**, 4096–4101 (2015).
4. Hansell, D. A. Recalcitrant dissolved organic carbon fractions. *Ann. Rev. Mar. Sci.* **5**, 421–445 (2013).
5. Follett, C. L., Repeta, D. J., Rothman, D. H., Xu, L. & Santinelli, C. Hidden cycle of dissolved organic carbon in the deep ocean. *Proc. Natl. Acad. Sci. USA.* **111**, 16706–16711 (2014).
6. Hansell, D. A. & Carlson, C. A. Deep-ocean gradients in the concentration of dissolved organic carbon. *Nature* **395**, 263–266 (1998).
7. Broecker, W. S. The great ocean conveyor belt drops hints before it slows. *Oceanographyography* **4**, 79–89 (1991).
8. Sulpis, O. et al. Respiration patterns in the Dark Ocean. *Glob. Biogeochem. Cycles* **37**, 1–21 (2023).
9. Hansell, D. A. & Carlson, C. A. Localized refractory dissolved organic carbon sinks in the deep ocean. *Glob. Biogeochem. Cycles* **27**, 705–710 (2013).
10. Kawabe, M., Fujio, S. & Yanagimoto, D. Deep-water circulation at low latitudes in the western North Pacific. *Deep. Res. Part I Oceanogr. Res. Pap.* **50**, 631–656 (2003).
11. Johnson, G. C. Deep water properties, velocities, and dynamics over ocean trenches. *J. Mar. Res.* **56**, 329–347 (1998).
12. Jiang, H. et al. Ocean circulation in the challenger deep derived from super-deep underwater glider observation. *Geophys. Res. Lett.* **48**, 1–11 (2021).
13. Tian, J. et al. A nearly uniform distributional pattern of heterotrophic bacteria in the Mariana Trench interior. *Deep. Res. Part I Oceanogr. Res. Pap.* **142**, 116–126 (2018).
14. Roussenov, V., Williams, R. G., Follows, M. J. & Key, R. M. Role of bottom water transport and diapycnic mixing in determining the radiocarbon distribution in the Pacific. *J. Geophys. Res. C. Ocean.* **109**, 1–18 (2004).
15. Bao, R. et al. Tectonically-triggered sediment and carbon export to the Hadal zone. *Nat. Commun.* **9**, 121 (2018).
16. Kioka, A. et al. Megathrust earthquake drives drastic organic carbon supply to the hadal trench. *Sci. Rep.* **9**, 1553 (2019).
17. Glud, R. N. et al. High rates of microbial carbon turnover in sediments in the deepest oceanic trench on Earth. *Nat. Geosci.* **6**, 284–288 (2013).
18. Zabel, M. et al. High carbon mineralization rates in subseafloor hadal sediments—Result of frequent mass wasting. *Geochem. Geophys. Geosyst.* **23**, e2022GC010502 (2022).
19. Leduc, D. et al. Comparison between infaunal communities of the deep floor and edge of the Tonga Trench: possible effects of differences in organic matter supply. *Deep. Res. Part I Oceanogr. Res. Pap.* **116**, 264–275 (2016).
20. Luo, M. et al. Benthic carbon mineralization in hadal trenches: insights from in situ determination of benthic oxygen consumption. *Geophys. Res. Lett.* **45**, 2752–2760 (2018).
21. Glud, R. N. et al. Hadal trenches are dynamic hotspots for early diagenesis in the deep sea. *Commun. Earth Environ.* **2**, 21 (2021).
22. Strasser, M., Ikehara, K., Everest, J. & Scientists, E. 386. *Japan Trench Paleoseismology. Proceedings of the International Ocean Discovery Program*. 386 (International Ocean Discovery Program, 2023).
23. Fujio, S. & Yanagimoto, D. Deep current measurements at 38° N east of Japan. *J. Geophys. Res.* **110**, C02010 (2005).
24. Ando, K., Kawabe, M. & Yanagimoto, D. Pathway and variability of deep circulation around 40°N in the northwest Pacific Ocean. *J. Oceanogr.* **69**, 159–174 (2013).
25. Ge, T. et al. Decadal variations in radiocarbon in dissolved inorganic carbon (DIC) along a transect in the Western North Pacific Ocean. *J. Geophys. Res. Ocean.* **127**, 1–17 (2022).
26. Shan, S. et al. Carbon cycling in the deep Mariana Trench in the western north Pacific Ocean: insights from radiocarbon proxy data. *Deep. Res. Part I Oceanogr. Res. Pap.* **164**, 103370 (2020).
27. Hansell, D. A. et al. *Compilation of Dissolved Organic Matter (DOM) Data Obtained from Global Ocean Observations from 1994 to 2021. Version 2 (NCEI Accession 0227166)* (NOAA National Centers for Environmental Information, 2021).
28. Owens, W. B. & Warren, B. A. Deep circulation in the northwest corner of the Pacific Ocean. *Deep. Res. Part I* **48**, 959–993 (2001).
29. Nozaki, Y. et al. The distribution of radionuclides and some trace metals in the water columns of the Japan and Bonin trenches. *Oceanol. Acta* **21**, 469–484 (1998).
30. Mitsuzawa, K. & Holloway, G. Characteristics of deep currents along trenches in the Northwest Pacific. *J. Geophys. Res. Ocean.* **103**, 85–92 (1998).
31. Druffel, E. R. M. et al. Dissolved organic radiocarbon in the central Pacific Ocean. *Geophys. Res. Lett.* **46**, 5396–5403 (2019).
32. Hansell, D. A., Carlson, C. A., Repeta, D. J. & Schlitzer, R. Dissolved organic matter in the ocean: a controversy stimulates new insights. *Oceanography* **22**, 202–211 (2009).
33. Kawagucci, S. et al. Hadal water biogeochemistry over the Izu-Ogasawara Trench observed with a full-depth CTD-CMS. *Ocean Sci.* **14**, 575–588 (2018).
34. Lin, H. T., Repeta, D. J., Xu, L. & Rappé, M. S. Dissolved organic carbon in basalt-hosted deep subseafloor fluids of the Juan de Fuca Ridge flank. *Earth Planet. Sci. Lett.* **513**, 156–165 (2019).
35. Loh, A. N., Bauer, J. E. & Druffel, E. R. M. Variable ageing and storage of dissolved organic components in the open ocean. *Nature* **430**, 877–881 (2004).
36. Fujio, S., Yanagimoto, D. & Taira, K. Deep current structure above the Izu-Ogasawara Trench. *J. Geophys. Res. Ocean.* **105**, 6377–6386 (2000).
37. Wang, J., Ma, Q., Wang, F., Lu, Y. & Pratt, L. J. Seasonal variation of the deep limb of the pacific meridional overturning circulation at yap-mariana junction. *J. Geophys. Res. Ocean.* **125**, e2019JC016017 (2020).
38. Shah Walter, S. R. et al. Microbial decomposition of marine dissolved organic matter in cool oceanic crust. *Nat. Geosci.* **11**, 334–339 (2018).

39. Santinelli, C., Follett, C., Retelletti Brogi, S., Xu, L. & Repeta, D. Carbon isotope measurements reveal unexpected cycling of dissolved organic matter in the deep Mediterranean Sea. *Mar. Chem.* **177**, 267–277 (2015).
40. Chu, M. et al. Earthquake-induced redistribution and reburial of microbes in the hadal trenches. *Innov. Geosci.* **1**, 100027 (2023).
41. LaBrie, R. et al. Deep ocean microbial communities produce more stable dissolved organic matter through the succession of rare prokaryotes. *Sci. Adv.* **8**, 1–13 (2022).
42. Chu, M. et al. Earthquake-enhanced dissolved carbon cycles in ultra-deep ocean sediments. *Nat. Commun.* **14**, 5427 (2023).
43. Kioka, A. et al. Event stratigraphy in a hadal oceanic trench: the Japan trench as sedimentary archive recording recurrent giant subduction zone earthquakes and their role in organic carbon export to the deep Sea. *Front. Earth Sci.* **7**, 319 (2019).
44. Keeling, C. D. The concentration and isotopic abundances of atmospheric carbon dioxide in rural areas. *Geochim. Cosmochim. Acta* **13**, 322–334 (1958).
45. Mortazavi, B. & Chanton, J. P. Use of Keeling plots to determine sources of dissolved organic carbon in nearshore and open ocean systems. *Limnol. Oceanogr.* **49**, 102–108 (2004).
46. DeMets, C., Gordon, R. G. & Argus, D. F. Geologically current plate motions. *Geophys. J. Int.* **181**, 1–80 (2010).
47. Nakamura, Y. et al. Incoming plate structure at the Japan Trench subduction zone revealed in densely spaced reflection seismic profiles. *Prog. Earth Planet. Sci.* **10**, 45 (2023).
48. Kioka, A. & Strasser, M. Oceanic Trenches. In *Treatise on Geomorphology* (ed. John (Jack) F. Shroder) 882–900 (Elsevier, 2022).
49. Ikehara, K. et al. Documenting large earthquakes similar to the 2011 Tohoku-oki earthquake from sediments deposited in the Japan Trench over the past 1500 years. *Earth Planet. Sci. Lett.* **445**, 48–56 (2016).
50. Xu, L. et al. Radiocarbon in dissolved organic carbon by UV oxidation: procedures and blank characterization at NOSAMS. *Radiocarbon* **63**, 357–374 (2021).
51. Xu, L. et al. Radiocarbon in dissolved organic carbon by UV oxidation: an update of procedures and blank characterization at NOSAMS. *Radiocarbon* **64**, 195–199 (2022).
52. van Geldern, R. et al. Stable carbon isotope analysis of dissolved inorganic carbon (DIC) and dissolved organic carbon (DOC) in natural waters - Results from a worldwide proficiency test. *Rapid Commun. Mass Spectrom.* **27**, 2099–2107 (2013).
53. Burdige, D. J., Komada, T., Magen, C. & Chanton, J. P. Modeling studies of dissolved organic matter cycling in Santa Barbara Basin (CA, USA) sediments. *Geochim. Cosmochim. Acta* **195**, 100–119 (2016).
54. Fu, W. et al. Carbon isotopic constraints on the degradation and sequestration of organic matter in river-influenced marginal sea sediments. *Limnol. Oceanogr.* **67**, S61–S75 (2022).
55. Walker, B. D., Beaupré, S. R., Griffin, S. & Druffel, E. R. M. UV photochemical oxidation and extraction of marine dissolved organic carbon at UC irvine: status, surprises, and methodological recommendations. *Radiocarbon* **61**, 1603–1617 (2019).
56. Bao, R., McNichol, A. P., McIntyre, C. P., Xu, L. & Eglinton, T. I. Dimensions of radiocarbon variability within sedimentary organic matter. *Radiocarbon* **60**, 775–790 (2018).
57. Longworth, B. E., Von Reden, K. F., Long, P. & Roberts, M. L. A high output, large acceptance injector for the NOSAMS tandetron AMS system. *Nucl. Instrum. Methods Phys. Res. Sect. B Beam Interact. Mater. At.* **361**, 211–216 (2015).
58. Gamo, T. & Shitashima, K. Chemical characteristics of hadal waters in the Izu-Ogasawara Trench of the western Pacific Ocean. *Proc. Jpn. Acad. Ser. B Phys. Biol. Sci.* **94**, 45–55 (2018).
59. Lauvset, S. K. et al. GLODAPv2.2022: the latest version of the global interior ocean biogeochemical data product. *Earth Syst. Sci. Data* **14**, 5543–5572 (2022).
60. Fofonoff, N. P. & Millard, R. C. Algorithms for computation of fundamental properties of seawater. *UNESCO Tech. Pap. Mar. Sci.* **44**, 53 (1983).
61. Masumoto, Y. et al. A fifty-year eddy-resolving simulation of the world ocean: preliminary outcomes of OFES (OGCM for the Earth Simulator). *J. Earth Simulator* **1**, 35–56 (2004).
62. Komori, N. et al. Description of sea-ice component of coupled ocean–sea-ice model for the earth simulator (OIFES). *J. Earth Simulator* **4**, 31–45 (2005).
63. Pacanowski, R. C. & Griffies, S. M. *The MOM3 Manual*. *GFDL Ocean Group Technical Report 4*. (Geophysical Fluid Dynamics Laboratory, 1999).
64. NOAA National Centers for Environmental Information. *ETOPO 2022 15 Arc-Second Global Relief Model*. https://doi.org/10.25921/fd45-gt74 (2022).
65. Druffel, E. R. M., Williams, P. M., Bauer, J. E. & Ertel, J. R. Cycling of dissolved and particulate organic matter in the open ocean. *J. Geophys. Res. Ocean.* **97**, 15639–15659 (1992).
66. Druffel, E. R. M. & Bauer, J. E. Radiocarbon distributions in Southern Ocean dissolved and particulate organic matter. *Geophys. Res. Lett.* **27**, 1495–1498 (2000).
67. Ding, L. et al. Radiocarbon in dissolved organic and inorganic carbon of the South China sea. *J. Geophys. Res. Ocean.* **125**, 1–14 (2020).
68. Druffel, E. R. M. et al. Dissolved organic radiocarbon in the eastern pacific and southern oceans. *Geophys. Res. Lett.* **48**, 1–9 (2021).
69. Bauer, J. E., Druffel, E. R. M., Wolgast, D. M., Griffin, S. & Masiello, C. A. Distributions of dissolved organic and inorganic carbon and radiocarbon in the eastern North Pacific continental margin. *Deep. Res. Part II Top. Stud. Oceanogr.* **45**, 689–713 (1998).
70. Tanaka, T., Otosaka, S., Wakita, M., Amano, H. & Togawa, O. Preliminary result of dissolved organic radiocarbon in the western North Pacific Ocean. *Nucl. Instrum. Methods Phys. Res. Sect. B Beam Interact. Mater. At.* **268**, 1219–1221 (2010).
71. Walker, B. D., Beaupré, S. R., Guilderson, T. P., Druffel, E. R. M. & McCarthy, M. D. Large-volume ultrafiltration for the study of radiocarbon signatures and size vs. age relationships in marine dissolved organic matter. *Geochim. Cosmochim. Acta* **75**, 5187–5202 (2011).

Acknowledgements

This research used samples and data provided by the International Ocean Discovery Program (IODP). We thank crew staffs and Dr. Nan Wang for assisting with sample preparation and measurement. We thank Drs. Ronnie N. Glud, Dennis A. Hansell, Matthias Zabel and Xin Xiao for their valuable suggestions. This research is supported by National Natural Science Foundation of China (Grants: 42450135, 92058207 and 42076037, R.B.), Taishan Young Scholars (Grant: tsqn202103030, R.B.), Shandong Natural Science Foundation (Grant: ZR2021JQ12, R.B.), and Fundamental Research Funds for the Central Universities (Grant: 202461018, M.C.).

Author contributions

R.B. designed this work with supervision from M.S., K.I., and E.D. All members of the IODP 386 Science Party contributed to sample acquirement, geochemical analysis and data collection. M.C., R.B., L.X., and K.L. conducted sample measurements. M.C., R.B., M. Liu., Y.D., and E.D. conducted data visualization. M.C. and R.B. drafted the figures and wrote the original draft. M.C., R.B., M.S., K.I., Y.D., K.L., M. Liu, L.X., Y.W., P.B., T.R., M.K., N.R., M. Luo, C.M., K.J., Z.C., C.M., and E.D. contributed to the interpretation of data and the editing of the manuscript.

Competing interests
The authors declare no competing interests.

Additional information
Supplementary information The online version contains supplementary material available at https://doi.org/10.1038/s41467-025-55883-1.

Correspondence and requests for materials should be addressed to Rui Bao.

Peer review information *Nature Communications* thanks Edgart Flores and the other, anonymous, reviewer(s) for their contribution to the peer review of this work. A peer review file is available.

Reprints and permissions information is available at http://www.nature.com/reprints

Publisher's note Springer Nature remains neutral with regard to jurisdictional claims in published maps and institutional affiliations.

Open Access This article is licensed under a Creative Commons Attribution-NonCommercial-NoDerivatives 4.0 International License, which permits any non-commercial use, sharing, distribution and reproduction in any medium or format, as long as you give appropriate credit to the original author(s) and the source, provide a link to the Creative Commons licence, and indicate if you modified the licensed material. You do not have permission under this licence to share adapted material derived from this article or parts of it. The images or other third party material in this article are included in the article's Creative Commons licence, unless indicated otherwise in a credit line to the material. If material is not included in the article's Creative Commons licence and your intended use is not permitted by statutory regulation or exceeds the permitted use, you will need to obtain permission directly from the copyright holder. To view a copy of this licence, visit http://creativecommons.org/licenses/by-nc-nd/4.0/.

© The Author(s) 2025